

1 **Ocean acidification over the next three centuries using a simple global climate carbon-cycle model:**
2 **projections and sensitivities.**

3

4 C. A. Hartin*, B. Bond-Lamberty, P. Patel and Anupriya Mundra

5

6 Pacific Northwest National Laboratory, Joint Global Change Research Institute at the University of

7 Maryland-College Park, 5825 University Research Court #3500, College Park, MD 20740, USA

8

9 *Corresponding author: Corinne.hartin@pnnl.gov

10

11 **ABSTRACT**

12 Continued oceanic uptake of anthropogenic CO₂ is projected to significantly alter the chemistry of the

13 upper oceans over the next three centuries, with potentially serious consequences for marine

14 ecosystems. Relatively few models have the capability to make projections of ocean acidification,

15 limiting our ability to assess the impacts and probabilities of ocean changes. In this study we examine

16 the ability of Hector v1.1, a reduced-form global model, to project changes in the upper ocean

17 carbonate system over the next three centuries, and quantify the model's sensitivity to parametric

18 inputs. Hector is run under prescribed emission pathways from the Representative Concentration

19 Pathways (RCPs) and compared to both observations and a suite of Coupled Model Intercomparison

20 (CMIP5) model outputs. Current observations confirm that ocean acidification is already taking place,

21 and CMIP5 models project significant changes occurring to 2300. Hector is consistent with the

22 observational record within both the high (>55°) and low latitude oceans (<55°). The model projects low

23 latitude surface ocean pH to decrease from preindustrial levels of 8.17 to 7.77 in 2100, and to 7.50 in

24 2300; aragonite saturation levels (Ω_{Ar}) decrease from 4.1 units to 2.2 in 2100 and 1.4 in 2300 under RCP

25 8.5. These magnitudes and trends of ocean acidification within Hector are largely consistent with the
26 CMIP5 model outputs, although we identify some small biases within Hector's carbonate system. Of the
27 parameters tested, changes in $[H^+]$ are most sensitive to parameters that directly affect atmospheric
28 CO_2 concentrations - Q_{10} (terrestrial respiration temperature response) as well as changes in ocean
29 circulation, while changes in Ω_{Ar} saturation levels are sensitive to changes in ocean salinity and Q_{10} . We
30 conclude that Hector is a robust tool well-suited for rapid ocean acidification projections, sensitivity
31 analyses, and is capable of emulating both current observations and large scale climate models under
32 multiple emission pathways.

33 **1. INTRODUCTION**

34 Human activities have led to increasing anthropogenic emissions of greenhouse gases to the
35 atmosphere. In the first decade of the 21st century CO₂ emissions from anthropogenic sources and land
36 use changes accounted for ~9 Pg C yr⁻¹, with future emission projections of up to 28 Pg C yr⁻¹ by 2100
37 under RCP 8.5 (Riahi et al., 2011). The world's oceans have played a critical role in lessening the effects
38 of climate change by absorbing 25-30% of the total anthropogenic carbon emissions since 1750 (Le
39 Quéré et al., 2013; Sabine et al., 2011).

40 In response to this increasing atmospheric burden of CO₂ and increasing oceanic uptake, the
41 oceans are experiencing both physical and biogeochemical changes: surface and deep water warming,
42 reduced subsurface oxygen, and a reduction in calcium carbonate saturation levels and pH (Doney,
43 2010). Mean surface ocean pH has already decreased by 0.1 units relative to preindustrial times
44 (Caldeira et al., 2003). If current emission trends continue, ocean acidification will occur at rates and
45 extents not observed over the last few million years (Feely et al., 2004; Feely et al., 2009; Kump et al.,
46 2009; Caldeira et al., 2003). Ocean acidification occurs when atmospheric CO₂ dissolves in seawater
47 (CO₂(aq)), forming carbonic acid (H₂CO₃); dissociating into carbonate (CO₃²⁻) and bicarbonate (HCO₃⁻),
48 and releasing protons (H⁺). The net effect of adding CO₂ to the system increases the concentrations of
49 [H₂CO₃], [HCO₃⁻], and [H⁺], while decreasing [CO₃²⁻] concentrations and lowering the pH. The sum of
50 [HCO₃⁻], [CO₃²⁻] and [CO₂^{*}], where [CO₂^{*}] = [CO₂(aq)] + [H₂CO₃] represents the dissolved inorganic (DIC) of
51 the system. As CO₂(aq) continues to increase in the ocean it reacts with CO₃²⁻, forming HCO₃⁻, decreasing
52 the fraction of CO₂ that can be readily absorbed by the oceans. Because of this capacity of the ocean to
53 buffer chemical changes, a doubling of atmospheric [CO₂] will not correspond to a doubling of [CO₂^{*}] but
54 instead will result in an increase on the order of 10% (Dickson and Millero, 1987). Due to both chemical
55 and physical changes (e.g., warming and stratification), the oceans may become less efficient in the

56 uptake of anthropogenic CO₂ as the climate continues to change (Sarmiento and Le Quéré, 1996; Matear
57 and Hirst, 1999; Joos et al., 1999; Le Quéré et al., 2010).

58 Numerous experiments and observations indicate that ocean acidification will have significant
59 effects on calcifying marine organisms. For example, the rate of coral reef building may decrease,
60 calcification rates of planktonic coccolithophores and foraminifera may be suppressed, and significant
61 changes in trophic level interactions and ecosystems may occur (Cooley and Doney, 2009; Silverman et
62 al., 2009; Fabry et al., 2008; Riebesell et al., 2000). Some coral reefs are believed to already be eroding
63 for parts of the year due to ocean acidification (Yates and Halley, 2006; Albright et al., 2013). Global
64 surface pH is projected to drop by up to 0.33 units (Gehlen et al., 2014; Orr et al., 2005) and all existing
65 coral reefs will be surrounded by conditions well outside of preindustrial values and even today's
66 saturation levels (Ricke et al., 2013) under the RCP8.5 scenario.

67 These model projections of ocean acidification come primarily from Earth System Models
68 (ESMs) that integrate the interactions of atmosphere, ocean, land, ice and biosphere to estimate the
69 present and future state of the climate. ESMs are computationally expensive and typically run using
70 stylized experiments or a few RCPs (greenhouse gas concentration trajectories used in the
71 Intergovernmental Panel on Climate Change 5th Assessment Report (IPCC, 2013)). This generally limits
72 ESM-based analyses to those scenarios. The occurrence of ocean warming and acidification is consistent
73 across CMIP5 ESMs, but their rates and magnitudes are strongly dependent upon the scenario (Bopp et
74 al., 2013).

75 An alternative to ESMs are reduced-form models, relatively simple and small models that can be
76 powerful tools due to their simple input requirements, computational efficiency, tractability, and thus
77 ability to run multiple simulations under arbitrary future emission pathways. This allows for the
78 quantification of arbitrary climate change scenarios, emulation of larger ESMs, as well as in-depth

79 parameter sensitivity studies and uncertainty analyses (Senior and Mitchell, 2000; Ricciuto et al., 2008;
80 Irvine et al., 2012).

81 Our goal of this study is to quantify how well Hector; a reduced-form model that explicitly treats
82 surface ocean chemistry; emulates the marine carbonate system of both observations and the CMIP5
83 archive; and explore the parametric sensitivities to Hector's ocean outputs. The remainder of the paper
84 is organized as follows; section 2, a detailed description of Hector's ocean component, the data sources
85 and simulations run, section 3, results of the model comparison and sensitivity experiments and lastly,
86 section 4, a discussion of the results.

87

88 **2 Model Description – Hector**

89 Hector is open-source and available at <https://github.com/JGCRI/hector>. The repository
90 includes all model code needed to compile and run the model, as well as all input files and R scripts to
91 process its output. Hector is a reduced form climate carbon-cycle model, which takes in emissions of
92 CO₂, non-CO₂s (e.g., CH₄, N₂O and halocarbons, and aerosols), converts emissions to concentrations
93 where needed, calculates the global radiative forcing, and then global mean temperature change.
94 Hector contains a well-mixed global atmosphere, a land component consisting of vegetation, detritus,
95 and soil, and an ocean component. In this study we use Hector v1.1, with an updated ocean
96 temperature algorithm to better match the CMIP5 mean. For a detailed description of the land and
97 atmospheric components of Hector, please refer to Appendix A and Hartin et al. (2015).

98 **2.1 Ocean Component**

99 Hector's ocean component is based on work by Lenton (2000), Knox and McElroy (1984) and
100 Sarmiento and Toggweiler (1984). It consists of four boxes: two surface boxes (high and low latitude),
101 one intermediate, and one deep box. The cold high latitude surface box makes up 15% of the ocean
102 surface area, representing the subpolar gyres (> 55°), while the warm low latitude surface box (<55°)

103 makes up 85% of the ocean surface area. The temperatures of the surface boxes are linearly related to
 104 the global atmospheric temperature change, and are initialized at 2°C and 22°C for the high and low
 105 latitude boxes respectively. This temperature gradient sets up a flux of carbon into the cold high latitude
 106 box and a flux out of the warm low latitude box. The ocean-atmosphere flux of carbon is the sum of all
 107 the surface fluxes (F_i , $n=2$).

$$F_O(t) = \sum_{i=1}^n F_i(t) \quad (1)$$

108 Once carbon enters the high latitude surface box it is circulated between the boxes via
 109 advection and water mass exchange, simulating a simple thermohaline circulation. In this version of
 110 Hector we do not explicitly model diffusion; simple box-diffusion models and “HILDA” (e.g., Siegenthaler
 111 and Joos, 1992) type models are typically in good agreement with observations but are more
 112 computationally demanding than a simple box model (Lenton, 2000). The change in carbon of any
 113 ocean box i is given by the fluxes in and out (j) with $F_{atm \rightarrow i}$ as the atmospheric carbon flux of the two
 114 surface boxes:

$$\frac{dC_i}{dt} = \sum_{j=1}^{in} F_{j \rightarrow i} - \sum_{j=1}^{out} F_{i \rightarrow j} + F_{atm \rightarrow i} \quad (2)$$

115 The flux of carbon between the boxes is related to the transport ($T_{i \rightarrow j}, m^3 s^{-1}$) between i and j , the
 116 volume of i (V_i, m^3), and the total carbon in i (including any air-sea fluxes) ($C_i, Pg C$):

$$\frac{dC_{i \rightarrow j}}{dt} = \frac{T_{i \rightarrow j} * C_i(t)}{V_i} \quad (3)$$

117 Volume transports are tuned to yield an approximate flow of 100 Pg C from the surface high latitude box
 118 to the deep ocean box at steady state, simulating deep water formation.

119 Hector calculates DIC, total alkalinity (TA), CO_3^{2-} , HCO_3^- , pCO_2 and pH. DIC and TA are the two
 120 carbonate variables used to solve the rest of the carbonate system. The detailed carbonate chemistry
 121 equations are based on numeric programs from Zeebe and Wolf-Gladrow, (2001) (Appendix B). We

122 simplified the equations by neglecting the effects of pressure, since we are only concerned with the
123 surface ocean. Hector is run to equilibrium in a perturbation-free mode, prior to running the historical
124 period, ensuring that it is in steady state (Hartin et al., 2015; Pietsch and Hasenauer, 2006). DIC (μmol
125 kg^{-1}) in the surface boxes is a function of the total carbon (Pg C) and the volume of the box. All carbon
126 within the ocean component is assumed to be inorganic carbon. Dissolved organic matter is less than
127 2% of the total inorganic carbon pool, of which a small fraction is dissolved organic carbon (Hansell and
128 Carlson, 2001) and particulate organic carbon less than 1% of the total carbon pool (Eglinton and
129 Repeta, 2004). Therefore, for simplicity we chose not to include dissolved or particulate organic carbon
130 within Hector.

131 TA is calculated at the end of model spinup (running to equilibrium in an a historical,
132 perturbation-free mode) and held constant throughout the run, resulting in 2311.0 $\mu\text{mol kg}^{-1}$ for the
133 high latitude box and 2435.0 $\mu\text{mol kg}^{-1}$ for the low latitude box. These values are within the range of
134 open ocean observations of 2250.0 – 2450.0 $\mu\text{mol kg}^{-1}$ (Key et al., 2004; Fry et al., 2015). We assume
135 negligible carbonate precipitation/dissolution and no alkalinity runoff from the land surface to the open
136 ocean. Alkalinity is typically held constant with time, which is a reasonable assumption over several
137 thousand years (Lenton, 2000; Zeebe and Wolf-Gladrow, 2001; Glotter et al., 2014; Archer et al., 2009).
138 On glacial-interglacial time scales alkalinity and the dissolution of CaCO_3 sediments is an important
139 factor in controlling atmospheric $[\text{CO}_2]$ (Sarmiento and Gruber, 2006), and thus on these scales Hector
140 will underestimate the oceanic CO_2 uptake.

141 Hector solves for pCO_2 , pH (total scale), and $[\text{HCO}_3^-]$, $[\text{CO}_3^{2-}]$, and aragonite (Ω_{Ar}) and calcite
142 saturation states (Ω_{Ca}) in both the high and low latitude surface ocean boxes. pCO_2 is calculated from the
143 concentration of $[\text{CO}_2^*]$ and the solubility of CO_2 in seawater, based on salinity and temperature. $[\text{CO}_2^*]$
144 is calculated from DIC and the first and second dissociation constants of carbonic acid from Mehrbach
145 et al. (1973), refit by Lueker et al. (2000) (Appendix B).

146 Carbon fluxes between the atmosphere and ocean are calculated (Takahashi et al., 2009):

$$F = k \alpha * \Delta pCO_2 = Tr * \Delta pCO_2 \quad (4)$$

147 where k is the CO_2 gas-transfer velocity, α is the solubility of CO_2 in seawater (K_0 , Appendix B), and the
148 ΔpCO_2 is the difference in pCO_2 between the atmosphere and ocean. The product of k and α results in
149 Tr , the sea-air gas transfer coefficient, where Tr ($g\ C\ m^{-2}\ month^{-1}\ \mu atm^{-1}$) = $0.585 * \alpha * Sc^{-1/2} * U_{10}^2$, 0.585
150 is a unit conversion factor (from $mol\ liter^{-1}\ atm^{-1}$ to $g\ C\ m^{-3}\ \mu atm^{-1}$ and from $cm\ h^{-1}$ to $m\ month^{-1}$) and Sc
151 is the Schmidt number. The Schmidt number (Appendix B) is calculated from Wanninkhof (1992) based
152 on the temperature of each surface box. The average wind speed (U_{10}) of $6.7\ m\ s^{-1}$ is the same over
153 both surface boxes (Table 1). pH (total scale), $[HCO_3^-]$, and $[CO_3^{2-}]$ are calculated using the $[H^+]$ ion and
154 solved for in a higher order polynomial (Appendix B).

155 Aragonite and calcite are the two primary carbonate minerals within seawater. The degree of
156 saturation in seawater with respect to aragonite (Ω_{Ar}) and calcite (Ω_{Ca}) is calculated from the product of
157 the concentrations of calcium $[Ca^{2+}]$ and carbonate ions $[CO_3^{2-}]$, divided by the solubility product (K_{sp}).
158 The $[Ca^{2+}]$ is based on equations from Riley and Tongudai (1967) at a constant salinity of 34.5. If $\Omega = 1$,
159 the solution is at equilibrium, and if $\Omega > 1$ ($\Omega < 1$) the solution is supersaturated (undersaturated) with
160 respect to the mineral.

$$\Omega = \frac{[Ca^{2+}][CO_3^{2-}]}{K_{sp}} \quad (5)$$

161 2.2. Simulation and experiments

162 Hector is run under prescribed emissions from 1850-2300 for all four Representative
163 Concentration Pathways (RCP 2.6, RCP 4.5, RCP 6, RCP 8.5) (Moss et al., 2010; van Vuuren et al., 2007).
164 We compare how well Hector can emulate the carbonate system of the CMIP5 median. Our results
165 section will mainly focus on RCP8.5 exploring the response of the carbonate system under a high
166 emissions scenario.

167 We also ran a series of model sensitivity experiments to quantify how influential some of
168 Hector's parameter inputs are on its outputs (in particular, $[H^+]$ and Ω_{Ar}). Such sensitivity analyses are
169 important to document model characteristics, explore model weaknesses, and determine to what
170 degree the model behavior conforms to our existing understanding of the ocean system. We do not
171 sample Hector's entire parameter space, a computationally demanding exercise, but instead choose a
172 list of the parameters that we expect, *a priori*, to be important in calculating the marine carbonate
173 system. We selected those parameters directly influencing atmospheric CO₂ concentrations (beta and
174 Q₁₀), parameters involved in the calculation of temperature (albedo and climate sensitivity) and those
175 parameters involved in the uptake of carbon in the surface ocean (ocean surface temperature, salinity,
176 wind stress, and ocean circulation). These parameters are varied by ±10% relative to the RCP8.5 control,
177 and we compare the percentage change from the reference and the perturbation cases in 2005, 2100,
178 and 2300. The reference, RCP8.5, refers to the tuned set of parameters found in Hector v1.1, resulting
179 in Figures 2-6.

180 **2.3 Data Sources**

181 All RCP input emission data are available at <http://tntcat.iiasa.ac.at/RcpDb/>. Comparison data are
182 obtained from a suite of CMIP5 Earth System Models (Table 2) (Taylor et al., 2012). The CMIP5 output is
183 available from the Program for Climate Model Diagnostics and Intercomparison
184 (<http://pcmdi3.llnl.gov/esgcet/home.htm>). We took the 0-100m (depth) mean for all available CMIP5
185 data for six output variables, computing the monthly mean for all years in the historical (1850-2005) and
186 RCP 8.5 (2006-2300) experiments. All outputs were regridded to a standard 1-degree grid using bilinear
187 interpolation in CDO version 1.7.1rc1, and then high latitude (-90 to -55 and 55 to 90 degrees), low
188 latitude (-55 to 55), and global area-weighted means computed using R 3.2.4. All CMIP5 comparisons
189 used in this study are from model runs with prescribed atmospheric CO₂ concentrations. We
190 acknowledge that this is not a perfect comparison, as Hector is emissions-forced being compared to the

191 concentration-forced CMIP5 models, but very few of the latter were run under prescribed emissions.
192 We use a combination of root mean square error (RMSE), rates of change (Δ) and bias (degree of
193 systematic over- or underestimation) to characterize Hector's performance relative to the CMIP5
194 median.

195 We also compare Hector to a series of observational ocean data. Surface ocean observations of
196 DIC, $p\text{CO}_2$, pH, Ω_{Ar} , and Ω_{Ca} are from time-series stations in both the high and latitude oceans; Hawaii
197 Ocean Time Series (HOT), Bermuda Atlantic Time Series (BATS), the European Station for Time Series in
198 the Ocean at the Canary Islands (ESTOC), the Irminger Sea, and the Iceland Sea (Table 3) . The time-
199 series data are annually averaged over the upper 100m of the water column. The carbonate parameters
200 not found in Table 3 are computed from temperature, salinity, and the given carbonate parameter pairs
201 using the CO2SYS software (Lewis and Wallace, 1998). The equilibrium constants (K1 and K2 from
202 Mehrbach et al., 1973 refit by Dickson and Millero, 1987) and zero total phosphorus and silica were
203 chosen to best match Hector. Lastly, a longer record (1708 – 1988) of pH and Ω_{Ar} from Flinder's Reef in
204 the western Coral Sea, calculated from boron isotope measurements, is used in the comparison
205 (Pelejero et al., 2005). We use rates of change (Δ) from 1988-2014, which overlaps the HOT and BATS
206 time series, to quantify how well Hector simulates the observed changes in the ocean carbonate
207 parameters (Table 6) (Dore et al., 2009; Bates et al., 2014).

208

209 **3. Results**

210 **3.1 Model and Observation Comparisons**

211 Hartin et al. (2015) conducted a thorough analysis of Hector v1.0 demonstrating that it can
212 reproduce the historical trends and future projections of atmospheric $[\text{CO}_2]$, radiative forcing, and global
213 temperature change under the four RCPs. In this study we focus on the upper ocean high and low
214 latitude inorganic carbon chemistry under RCP 8.5.

215 Hector captures the trend in DIC concentrations for both the high and low latitude surface
216 ocean with a global RMSE average of $7.0 \mu\text{mol kg}^{-1}$ when compared to CMIP5 models over the historical
217 period (Table 4; Figure 2). We note that there is a systematic bias in both the high and low latitude
218 surface boxes when compared to CMIP5. First, the carbon pools of the surface boxes are initialized with
219 carbon values slightly higher than the median CMIP5 values. Second, after 2100 the high latitude CMIP5
220 median begins to decline, while Hector rises and stabilizes. Only 3 CMIP5 models ran out to 2300, with
221 one model driving the decline. Regardless, this offset only results in a <3% global difference between
222 CMIP5 and Hector.

223 Hector accurately tracks the pCO_2 in both the high and low latitude surface ocean with similar
224 rates of change from 1850-2300 (Figure 3). There is a low bias in Hector compared to CMIP5 models
225 after 2100, due to the low bias in projected atmospheric $[\text{CO}_2]$ within Hector over the same time period
226 (Hartin et al., 2015). We do find Hector to be in closer agreement with the observation record.

227 Figure 4 shows the high and low latitude surface pH of Hector compared to CMIP5 and
228 observations from BATS, HOT, ESTOC, Irminger Sea, Iceland Sea, and Flinders Reef. While the high
229 latitude surface pH is slightly higher than the CMIP5 models, Hector is more similar to high latitude
230 observations. Since the preindustrial, observations of surface ocean pH decreased by 0.08 units,
231 corresponding to a 24% increase in $[\text{H}^+]$ concentrations and an 8% decrease in $[\text{CO}_3^{2-}]$, similar to
232 numerous studies (Feely et al., 2004; Sabine et al., 2004; Caldeira et al., 2003; Orr et al., 2005) that
233 estimate an average global decrease in pH of 0.1 or a 30% increase in $[\text{H}^+]$.

234 The Flinder's Reef pH record provides a natural baseline to compare future trends in ocean
235 acidification. While we did not expect the model to match exactly, as this reef site is heavily influenced
236 by coastal dynamics and internal variability, rates of change from the preindustrial (1750) to 1988 are
237 the same (0.0002 yr^{-1}) for both Hector and Flinder's Reef. Over the limited observational record from
238 both the Pacific and Atlantic Oceans, Hector accurately simulates the decline in pH (-0.0017 yr^{-1})

239 compared to observations (Table 6). Other observations in the North Pacific show surface changes of
240 pH up to 0.06 units between 1991 and 2006 with an average rate of -0.0017 yr^{-1} (Byrne et al., 2010).
241 Recent work suggests that the North Atlantic absorbed 50% more anthropogenic CO_2 in the last decade
242 compared to the previous decade, decreasing surface pH by 0.0021 (Woosley et al., 2016). Under RCP
243 8.5, Hector projects a decrease in low latitude pH of 8.17 in 1850 to 7.77 in 2100 and down to 7.5 by
244 2300, similar to CMIP5 (Table 5). At approximately 2050, atmospheric $[\text{CO}_2]$ is twice the preindustrial
245 concentrations, corresponding to a decrease in pH to 7.96. Shortly after this doubling, pH values are
246 well outside the natural variability found in Flinder's Reef.

247 Figure 5 illustrates the high and low latitude surface Ω_{Ar} . We only highlight Ω_{Ar} , as Ω_{Ca} is similar
248 to that of Ω_{Ar} . As with pH, Hector is slightly higher than the CMIP5 Ω_{Ar} median but closer to the
249 observational record. Hector accurately simulates the change in Ω_{Ar} (-0.0090 yr^{-1}) compared to
250 observations (Table 6). Repeated oceanographic surveys in the Pacific Ocean have observed an average
251 $0.34\% \text{ yr}^{-1}$ decrease in the saturation state of surface seawater with respect to aragonite and calcite over
252 a 14-year period (1991-2005) (Feely et al., 2012); the average decrease in Hector is between $0.19\% \text{ yr}^{-1}$
253 and $0.25\% \text{ yr}^{-1}$. Saturation levels of Ω_{Ar} decrease rapidly over the next 100 years in both the high and
254 low latitude. Hector accurately captures the decline in saturation states with low RMSE values for Ω_{Ar} .
255 Under RCP8.5 Hector projects that low latitude Ω_{Ar} will decrease to 2.2 by 2100 and down to 1.4 by
256 2300. The high latitude oceans will be undersaturated with respect to aragonite by 2100 and will drop
257 down to 0.7 by 2300.

258 Lastly, Figure 6 highlights pH and Ω_{Ar} projections under all four RCPs from 1850 to 2300. Over
259 the last 20 years, both pH and Ω_{Ar} have declined sharply and will continue to decline under RCP 4.5, 6.0
260 and 8.5, outside of their preindustrial and present day values. These RCPs represent a range of possible
261 future scenarios, with ocean pH varying between 8.15 and 7.46 for the high latitude and Ω_{Ar} varying
262 between 1.94 and 0.60. High latitude Ω_{Ar} saturation levels presently are much lower than the low

263 latitude and reach undersaturation before the end of the century. Even under a best-case scenario, RCP
264 2.6, low latitude pH will drop to 8.07 by 2100 and to 8.12 by 2300, with Ω_{Ar} saturation states remaining
265 well outside of present day values.

266 **3.2 Model Parameter Sensitivity**

267 Parametric sensitivities are different between $[H^+]$ and Ω_{Ar} . We use $[H^+]$ to highlight changes in
268 pH, as $pH = -\log[H^+]$. In the near term (from 2005-2100) the calculation of pH is sensitive to a
269 combination of parameters, ocean circulation, beta (terrestrial CO_2 fertilization), and wind stress, while
270 on longer time scales (to 2300), $[H^+]$ is most sensitive to changes in Q_{10} (terrestrial respiration
271 temperature response) and ocean circulation (Table 7). Global Ω_{Ar} is most sensitive to changes in
272 salinity in both the near and long term. Similar to $[H^+]$, Ω_{Ar} becomes more sensitive to changes in Q_{10} in
273 the long term.

274

275 **4. Discussion**

276 The marine carbonate system is projected to undergo significant changes under the RCPs. pCO_2
277 and DIC are increasing rapidly as atmospheric $[CO_2]$ continues to rise under RCP 4.5, 6.0 and 8.5. pH, and
278 Ω_{Ar} are decreasing rapidly outside of observations and are projected to continue to decrease under all
279 scenarios (Figure 6). Only under RCP 2.6 do pH and Ω_{Ar} values begin to increase towards present day
280 values. A lowering of Ω_{Ar} from approximately 4.0 to 3.0 is predicted to lead to significant reductions in
281 calcification rates in tropical reefs (Kleypas et al., 1999; Silverman et al., 2009). By the end of the 21st
282 century low latitude ocean Ω_{Ar} will drop below 3.0, well outside of the preindustrial values of $\Omega_{Ar} > 3.5$,
283 and high latitude ocean Ω_{Ar} is close to undersaturation ($\Omega < 1$) (Figure 6). These results agree with other
284 studies that investigated changes to the carbonate system (Roy et al., 2015; Rieke et al., 2013).
285 Accounting for seasonal variations in the Ω_{Ar} saturation levels the time of undersaturation may move
286 forward by up to 17 ± 10 years (Sasse et al., 2015). Due to Hector's time step of 1 year, we may be

287 overestimating the time when ocean acidification reaches a critical threshold. We also note that other
288 factors such as eutrophication, river discharge, and upwelling will likely increase the probability that
289 coastal regions will experience the effects of ocean acidification sooner than the projected open ocean
290 values in Hector (Ekstrom et al., 2015).

291 Using $[H^+]$ as a proxy for pH, we find that $[H^+]$ is sensitive to Q_{10} and ocean circulation. Changes
292 in Q_{10} , (the respiration temperature response) is responsible for the release of carbon on land.
293 Uncertainties in the land carbon cycle have been attributed to uncertainties in future CO_2 projections
294 within the CMIP5 models (Friedlingstein et al., 2014). Therefore, uncertainties in the land carbon cycle
295 will also have implications for the marine carbonate system. A 10% change in the thermohaline
296 circulation parameter (Tt in Figure 1), representing a portion of the high latitude to deep ocean
297 circulation, results in $\sim 3\%$ change in $[H^+]$. The dynamics of ocean uptake of CO_2 are strongly dependent
298 on this circulation of CO_2 laden waters from the surface ocean to depth. CMIP5 models project a
299 weakening in the Atlantic meridional overturning circulation by an average of 36% under RCP8.5 by 2100
300 (Cheng et al., 2013). Therefore, changes in ocean circulation may have implications on the marine
301 carbonate system, influencing the ocean pH. We also find that the high latitude surface ocean is more
302 sensitive to parameter changes than the low latitude surface ocean. The high latitude box makes up 15%
303 of the global oceans in Hector and therefore, changes of the same size are more easily felt in the high
304 latitude box compared to the low latitude box. This may have direct implications on future marine
305 carbonate projections.

306 Global Ω_{Ar} saturation levels are most sensitive to changes in salinity. Salinity is used to calculate
307 $[Ca^{2+}]$ and total boron (Appendix B). Typically the carbonate system is normalized to changes in salinity
308 to understand the chemical changes within the system, instead we show that Ω_{Ar} may be sensitive not
309 only to future changes in atmospheric $[CO_2]$ but also sensitive to changes in precipitation and

310 evaporation. This may be important, as studies suggest significant changes in precipitation patterns
311 under a changing climate (Held and Soden, 2006; Liu and Allan, 2013).

312

313

314 **5. Conclusions**

315 We developed a simple, open-source, object oriented carbon cycle climate model, Hector, that
316 reliably reproduces the median of the CMIP5 climate variables (Hartin et al., 2015). The ocean
317 component presented in this study calculates the upper ocean carbonate system ($p\text{CO}_2$, DIC, pH, Ω_{Ar} ,
318 Ω_{Ca}). Under all four RCPs, pH and Ω_{Ar} decrease significantly outside of their preindustrial values
319 matching both observations and CMIP5. In the near future the open ocean and coral reef communities
320 are likely to experience pH and carbonate saturation levels unprecedented in the last 2 million years
321 (Hönisch et al., 2009).

322 This study is timely because the CMIP5 archive includes a large suite of ESMs that contained
323 dynamic biogeochemistry, allowing us to study future projections of the marine carbon cycle. Rather
324 than running the ESMs, we can use Hector to quickly emulate the global CMIP5 median for projection
325 studies under different emission pathways and sensitivity analyses of the marine carbonate system.
326 Within this study we find that numerous parameters influence $[\text{H}^+]$ and Ω_{Ar} , with both being sensitive to
327 Q_{10} . Due to Hector's simplistic nature and fast execution times, Hector has the potential to be a critical
328 tool to the decision-making, scientific, and integrated assessment communities, allowing for further
329 understanding of future changes to the marine carbonate system.

330 **Appendix A: Model Description – carbon cycle**

331 The carbon component in Hector contains three carbon reservoirs: a single well-mixed atmosphere,
332 a land component and an ocean component. The change in atmospheric carbon is a function of the
333 anthropogenic emissions (F_A), land-use change emissions (F_{LC}), and atmosphere-ocean (F_O) and
334 atmosphere-land (F_L) carbon fluxes. The default model time step is 1 year.

$$\frac{dC_{atm}(t)}{dt} = F_A(t) + F_{LC}(t) - F_O(t) - F_L(t) \quad (1)$$

335 The terrestrial cycle in Hector contains vegetation, detritus, and soil, all linked to each other and
336 the atmosphere by first-order differential equations. Vegetation net primary production is a function of
337 atmospheric CO_2 and temperature. Carbon flows from the vegetation to detritus to soil and loses
338 fractions of carbon to heterotrophic respiration on the way. An ‘earth’ pool debits carbon emitted as
339 anthropogenic emissions, allowing a continual mass-balance check across the entire carbon cycle.

340 Atmosphere-land fluxes at time t are calculated by:

$$F_L(t) = \sum_{i=1}^n NPP_i(t) - RH_i(t) \quad (2)$$

341 where NPP is the net primary production and RH is the heterotrophic respiration summed over user-
342 specified n groups (i.e., latitude bands, political units, or biomes) (Hartin et al 2015).

343

344 **Appendix B: Ocean Carbonate Chemistry**

345 The ocean’s inorganic carbon system is solved via a series of equations modified from Zeebe and Wolf-
346 Gladrow (2001). TA and DIC are used to calculate the other variables of the carbonate system:

$$DIC * \left(\frac{K_1}{[H^+]} + 2 \frac{K_1 K_2}{[H^+]^2} \right) = \left(TA - \frac{K_B B_T}{K_B + [H^+]} - \frac{K_W}{[H^+]} + [H^+] \right) * \left(1 + \frac{K_1}{[H^+]} + \frac{K_1 K_2}{[H^+]^2} \right) \quad (1)$$

347 This equation results in a higher order polynomial equation for H^+ , in which the roots (1 positive, 4
348 negative) are solved for. Once H^+ is solved for, pH , pCO_2 , HCO_3^- , and CO_3^{2-} can be determined. We

349 ignore the nonideality of CO₂ in air and therefore use the partial pressure of CO₂ instead of the fugacity
 350 of CO₂. Fugacity is slightly lower by ~0.3% compared to pCO₂ (Riebesell et al., 2009; Sarmiento and
 351 Gruber, 2006).

$$[CO_2^*] = \frac{DIC}{\left(1 + \frac{K_1}{[H^+]} + \frac{K_1 K_2}{[H^+]^2}\right)} \quad (2)$$

$$pCO_2 = \frac{[CO_2^*]}{K_H} \quad (3)$$

$$[HCO_3^-] = \frac{DIC}{\left(1 + \frac{[H^+]}{K_1} + \frac{K_2}{[H^+]}\right)} \quad (4)$$

$$[CO_3^{2-}] = \frac{DIC}{\left(1 + \frac{[H^+]}{K_2} + \frac{[H^+]^2}{K_1 K_2}\right)} \quad (5)$$

$$K_1 = \frac{[H^+][HCO_3^-]}{[CO_2]} \quad (6)$$

$$K_2 = \frac{[H^+][CO_3^{2-}]}{[HCO_3^-]} \quad (7)$$

352 K₁ and K₂ are the first and second acidity constants of carbonic acid from Mehrbach et al. (1973) and
 353 refit by Lueker et al. (2000).

$$K_B = \frac{[H^+][B(OH)_4^-]}{[B(OH)_3]} \quad (8)$$

354 K_B is the dissociation constant of boric acid from DOE (1994).

$$B = 416.0 * \frac{S}{35.0} \quad (9)$$

356 Total boron is from DOE (1994)

$$K_W = \frac{[H^+]}{[OH^-]} \quad (10)$$

357 K_w is the dissociation constant of water from Millero (1995).

$$K_{sp} = [Ca^{2+}] * [CO_3^{2-}] \quad (11)$$

358 K_{sp} of aragonite and calcite is calculated from Mucci, (1983).

359

360 For those equations with multiple coefficients:

361 1) K_H and K_0 are similar equations calculating Henry's constant or the solubility of CO_2 , but they return
362 different units ($mol\ kg^{-1}\ atm^{-1}$ and $mol\ L^{-1}\ atm^{-1}$) (see Weiss, 1974 for equations and coefficients). K_H
363 is used to solve pCO_2 while K_0 is used to solve air-sea fluxes of CO_2 .

364 2) The Schmidt number is taken from Wanninkhof (1992) for coefficients of CO_2 in seawater.

365 3) $[Ca^{2+}]$ ($mol\ kg^{-1}$) is calculated from Riley and Tongudai (1967).

366

367 **Acknowledgements**

368 This research is based on work supported by the US Department of Energy. The Pacific Northwest
369 National Laboratory is operated for DOE by Battelle Memorial Institute under contract DE-AC05-
370 76RL01830.

371

372 **Author Contributions**

373 C.Hartin designed and carried out the experiments. C. Hartin, B.Bond-Lamberty, and P.Patel
374 developed the model code. A.Mundra processed the data and prepared the figures. C.Hartin
375 prepared the manuscript with contributions from all co-authors.

376

377 **Table 1:** Description and values of ocean parameters in Hector and parameters involved in the
 378 sensitivity analysis.

Description	Value	Notes
*Albedo ^t	-0.2 Wm ⁻²	Constant global albedo from 1950 - 2300
Area of ocean	3.6e14 m ²	Knox and McElroy, (1984)
*Beta ^t	0.36	Terrestrial CO ₂ fertilization Wullschleger et al. (1995)
*Climate Sensitivity ^t	3.0 °C	
Fractional area of HL	0.15	Sarmiento and Toggweiler, (1984)
Fractional area of LL	0.85	Sarmiento and Toggweiler, (1984)
*Q ₁₀ ^t	2.0	Terrestrial respiration temperature response Davidson and Janssens (2006)
Thickness of surface ocean	100 m	Knox and McElroy, (1984)
Thickness of intermediate ocean	900 m	
Thickness of deep ocean	2677 m	Total ocean depth 3777m
Volume of HL	5.4e15 m ³	
Volume of LL	3.06e16 m ³	
Volume of IO	3.24e17 m ³	
Volume of DO	9.64e17 m ³	
Surface Area of HL	5.4e13 m ²	
Surface Area of LL	3.06e14 m ²	
Salinity HL and LL ^l	34.5	
Initial temperature of HL ^l	2.0 °C	

Initial temperature of LL [†]	22.0 °C	
*Thermohaline circulation (T _T) [‡]	7.2e7 m ³ s ⁻¹	Tuned to give ~100 Pg C flux from surface to deep
*High latitude circulation (T _H)	4.9e7 m ³ s ⁻¹	Tuned to give ~100 Pg C flux from surface to deep
*Water mass exchange (intermediate to deep - E _{ID})	1.25e7 m ³ s ⁻¹	Lenton (2000); Knox and McElroy (1984)
*Water mass exchange (low latitude to intermediate - E _{IL})	2.08e7 m ³ s ⁻¹	Lenton (2000); Knox and McElroy (1984)
Wind speed HL and LL [†]	6.7 m s ⁻¹	Takahashi et al. (2009); Liss and Merlivat, (1986)

379 * Parameters contained within the input file.

380 [†] Parameters varied for the sensitivity analysis.

381 **Table 2:** CMIP5 ESM models used in this study containing ocean carbonate parameters. Ω_{Ar} , Ω_{Ca} were
 382 calculated from the model sea surface temperature, sea surface salinity, and CO_3 concentrations.

Model	Parameters (RCP 8.5)
BCC-cm1-1	pCO ₂ [*] , temperature
BNU-ESM	pCO ₂
CanESM2	DIC, pH, salinity
CESM1-BGC	CO ₃ , DIC, pH, salinity
CMCC-CESM	pCO ₂ , temperature, CO ₃ , DIC, pH, salinity
CNRM-CM5	CO ₃ , DIC
GFDL-ESM2G	pCO ₂ , temperature, pH, salinity
GFDL-ESM2M	pCO ₂ , temperature, CO ₃ , pH, DIC, salinity
GISS-E2-H-CC	pCO ₂ , temperature, DIC, salinity
GISS-E2-R-CC	pCO ₂ , temperature, DIC, salinity
HadGEM2-CC	pCO ₂ , temperature, CO ₃ , DIC, pH, salinity
HadGEM2-ES	pCO ₂ , temperature, CO ₃ [*] , DIC [*] , pH, salinity
IPSL-CM5A-LR	Temperature [*] , CO ₃ [*] , DIC [*] , pH [*] , salinity [*]
IPSL-CM5A-MR	Temperature, CO ₃ , DIC, pH, salinity
IPSL-CM5B-LR	Temperature, CO ₃ , DIC, pH, salinity
MIROC-ESM	pCO ₂ , temperature, salinity
MIROC-ESM- CHEM	pCO ₂ , temperature, salinity
MPI-ESM-LR	pCO ₂ [*] , temperature [*] , CO ₃ [*] , DIC [*] , pH [*] , salinity [*]
MPI-ESM-MR	pCO ₂ , temperature, CO ₃ , DIC, pH, salinity
MRI-ESM1	pCO ₂ , temperature
NorESM1-ME	pCO ₂ , temperature, CO ₃ , DIC, pH, salinity

383 * Variable output to 2300.

384 **Table 3:** Observational time-series information and carbonate parameters from each location.
 385

Time-Series Site	Location	Time-Series Length	Reference	Ocean Carbon Parameters	Data Access
BATS	Sargasso Sea	1988-2011	Bates, (2007)	TA, DIC	http://www.bios.edu/research/projects/bats
HOT	North Pacific	1988-2011	Dore et al. (2009)	TA, DIC, pH, pCO ₂ , Ω_{Ar} , Ω_{Ca}	http://hahana.soest.hawaii.edu/hot/hot_jgofs.html
ESTOC	Canary Islands	1995-2009	Gonzalez-Davila, (2009)	TA, pH, pCO ₂	http://www.eurosites.info/estoc.php
Iceland Sea	Iceland Sea	1985-2013	Olafsson, (2007a)	DIC, pCO ₂	http://cdiac.ornl.gov/oceans/Mooring/Iceland_Sea.html
Irminger Sea	Irminger Sea	1983-2013	Olafsson, (2007b)	DIC, pCO ₂	http://cdiac.ornl.gov/oceans/Mooring/Irminger_Sea.html
Flinders Reef	Coral Sea	1708-1988	Pelejero et al. (2005)	pH, Ω_{Ar}	ftp://ftp.ncdc.noaa.gov/pub/data/paleo/coral/west_pacific/great_barrier/flinders2005.txt

386

387 **Table 4:** Model validation metrics for the a) high latitude and b) low latitude ocean carbonate variables
 388 comparing Hector to CMIP5 from 1850-2005.
 389

a)	RMSE	R2	Bias
DIC	10.00	0.26	47.10
pCO ₂	2.65	0.98	-31.78
pH	0.004	0.975	0.061
Ω _{Ar}	0.01	0.98	0.37
Ω _{Ca}	0.02	0.98	0.58

b)	RMSE	R2	Bias
DIC	6.50	0.76	101.28
pCO ₂	3.43	0.98	-4.62
pH	0.004	0.966	0.025
Ω _{Ar}	0.02	0.97	0.36
Ω _{Ca}	0.03	0.97	0.53

390
 391
 392
 393
 394
 395

Table 5: Absolute values and rates of change per year (Δ) for the a) high and b) low latitude surface ocean from 1850-2100 and 2101-2300 under RCP 8.5 for DIC (μmol kg⁻¹), pCO₂ (μatm), pH (total scale, unitless), Ω_{Ar} (unitless) and Ω_{Ca} (unitless).

a)	DIC			pCO ₂			pH			Ω _{Ar}			Ω _{Ca}		
	1850	2100	2300	1850	2100	2300	1850	2100	2300	1850	2100	2300	1850	2100	2300
Hector	2107.5	2258.1	2335.5	244.7	816.6	1732.1	8.23	7.76	7.46	2.2	1.0	0.6	3.5	1.5	0.9
Δ		0.602	0.387		2.29	4.58		-	-		-	-0.002		-0.008	-0.003
								0.0019	0.0015		0.0048				
CMIP5	2104.50	2175.79	2243.41	271.62	871.00	1903.82	8.17	7.70	7.38	1.82	0.75	0.44	2.90	1.20	0.70
Δ		0.285	0.34		2.40	5.16		-	-		-	-		-	-
								0.0019	0.0016		0.0012	0.0016		0.0068	0.0025

396

b)	DIC			pCO ₂			pH			Ω _{Ar}			Ω _{Ca}		
	1850	2100	2300	1850	2100	2300	1850	2100	2300	1850	2100	2300	1850	2100	2300
Hector	2073.9	2264.1	2357.6	294.7	879.6	1766.5	8.17	7.77	7.50	4.1	2.2	1.4	6.2	3.3	2.1
Δ		0.76	0.47		2.34	4.43		-	-		-	-		-	-0.006
								0.0016	0.0014		0.0076	0.0040		0.0116	
CMIP5	1997.57	2163.16	2298.89	290.47	930.92	1965.23	8.16	7.73	7.45	3.75	2.00	1.36	5.77	3.02	2.04
Δ		0.66	0.68		2.56	5.17		-	-		-	-		-	-0.0049
								0.0011	0.0014		0.0070	0.0032		0.0110	

397

398 **Table 6:** Trends and standard error for the carbonate system taken from Bates et al. (2014) and values
 399 calculated from Hector and CMIP5.
 400

	Length of record	DIC ($\mu\text{mol kg}^{-1} \text{yr}^{-1}$)	pCO ₂ ($\mu\text{atm yr}^{-1}$)	pH (yr^{-1})	Ω_{Ar} (yr^{-1})
BATS	1983-2014	1.37 ± 0.07	1.69 ± 0.11	-0.0017 ± 0.0001	-0.0095 ± 0.0007
HOT	1988-2014	1.78 ± 0.12	1.72 ± 0.09	-0.0016 ± 0.0001	-0.0084 ± 0.0011
ESTOC	1995-2014	1.09 ± 0.10	1.92 ± 0.24	-0.0018 ± 0.0002	-0.0115 ± 0.0023
Iceland Sea	1983-2014	1.22 ± 0.27	1.29 ± 0.36	-0.0014 ± 0.0005	-0.0018 ± 0.0027
Irminger Sea	1983-2014	1.62 ± 0.35	2.37 ± 0.49	-0.0026 ± 0.0006	-0.0080 ± 0.0040
Hector	1988-2014	0.90	1.82	-0.0017	-0.0089
CMIP5	1988-2014	0.68	1.77	-0.0018	-0.0074

401
 402

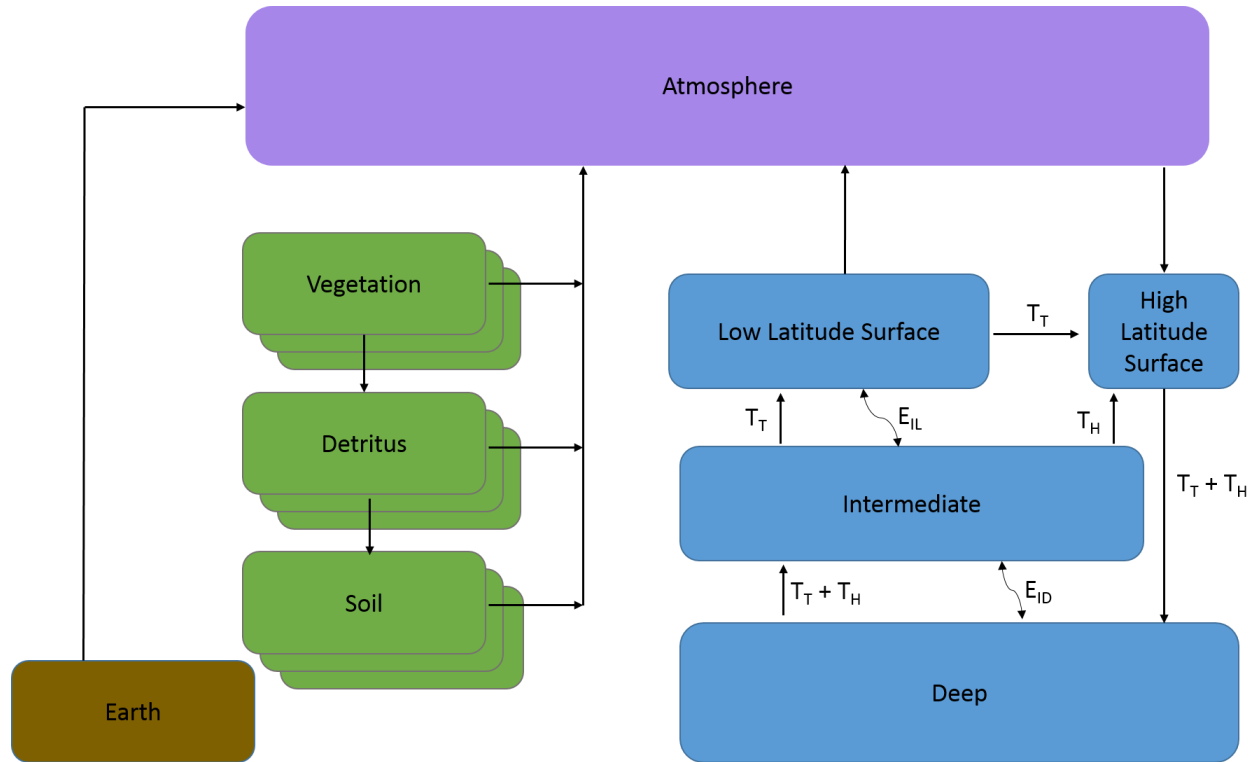
403 **Table 7:** Percentage change from reference (RCP8.5) for two Hector outputs a) global $[H^+]$ and b) global
 404 Ω_{Ar} for a $\pm 10\%$ change in eight model parameters. Results are shown for three years, 2005, 2100 and
 405 2300.
 406

a) Year	Parameter	+10% change	-10% change
2005	Albedo	0.13	0.00
2100		0.59	0.00
2300		0.00	-0.31
2005	Beta (terrestrial CO ₂ fertilization)	0.63	-0.50
2100		1.78	-1.78
2300		1.56	-1.88
2005	Ocean Circulation (T_T)	0.76	-0.76
2100		2.37	-1.78
2300		2.81	-3.44
2005	Q_{10} (terrestrial respiration temperature response)	-0.13	0.13
2100		-0.59	1.18
2300		-3.13	3.44
2005	Salinity	-0.88	1.51
2100		0.59	0.59
2300		1.88	-1.25
2005	Climate Sensitivity	-0.13	0.13
2100		-0.59	0.43
2300		-2.5	2.50
2005	Surface ocean temperature	0.00	0.00
2100		0.00	0.59
2300		0.62	0.31
2005	Wind Stress	-0.38	0.63
2100		-0.59	1.78
2300		-1.25	1.25

407

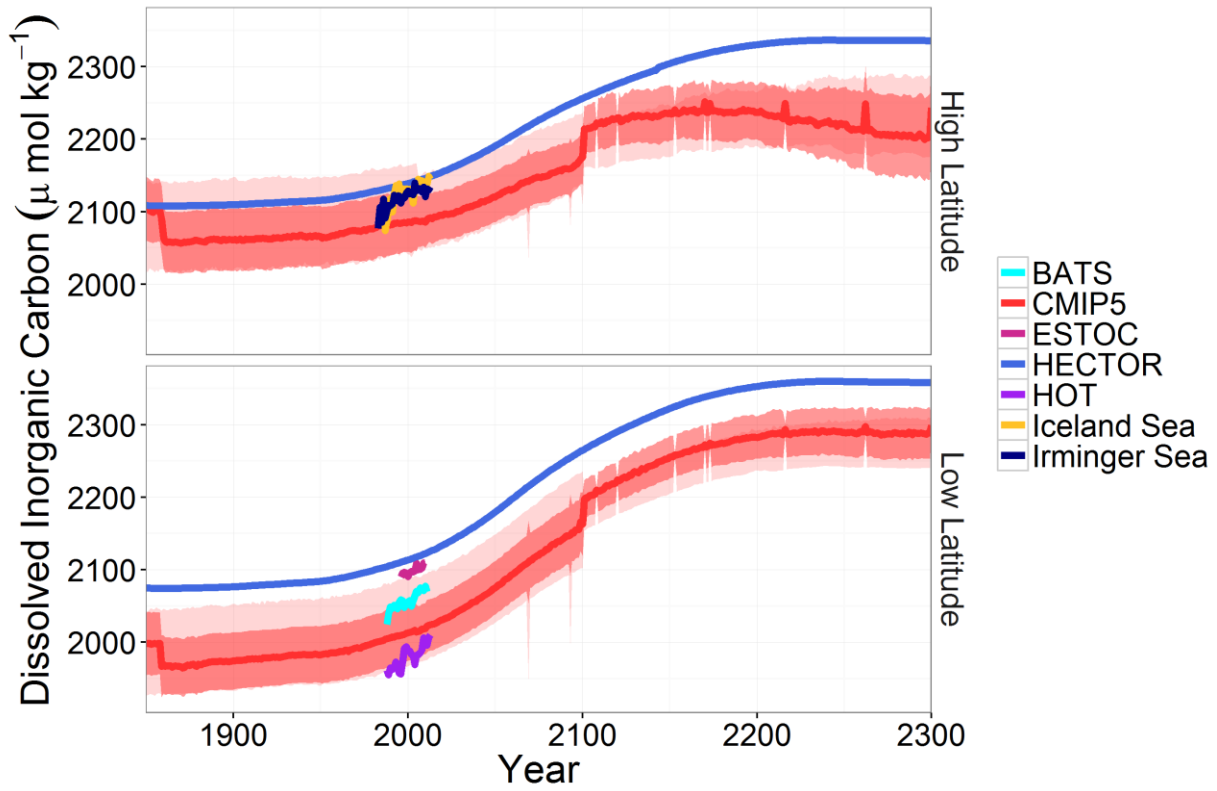
b) Year	Parameter	+10% change	-10% change
2005	Albedo	0.01	-0.00
2100		0.01	-0.01
2300		-0.00	0.00
2005	Beta (terrestrial CO ₂ fertilization)	0.38	-0.40
2100		1.33	-1.34
2300		1.38	-1.35
2005	Ocean Circulation (T _T)	0.41	-0.45
2100		1.01	-1.05
2300		1.48	-1.55
2005	Q ₁₀ (terrestrial respiration temperature response)	-0.09	0.10
2100		-0.87	0.95
2300		-2.40	3.00
2005	Salinity	3.80	-4.28
2100		5.60	-5.89
2300		7.17	-7.18
2005	Climate Sensitivity	0.07	-0.07
2100		0.55	-0.56
2300		0.43	-0.27
2005	Surface ocean temperature	2.07	-1.99
2100		2.41	-2.29
2300		2.43	-2.27
2005	Wind Stress	-0.18	0.25
2100		-0.65	0.88
2300		-1.13	0.88

409 **Figure 1:** Representation of the carbon cycle in Hector. The atmosphere consists of one well-mixed box,
 410 connected to the surface ocean via air-sea fluxes of carbon. The terrestrial component consists of user
 411 defined biomes or regions for vegetation, detritus, and soil. The earth pool is continually debited to act
 412 as a mass balance check on the carbon cycle (Hartin et al., 2015). The ocean consists of four boxes, with
 413 advection (represented by straight arrows) and water mass exchange (represented by curved arrows)
 414 simulating thermohaline circulation. The marine carbonate system is solved for in the high and low
 415 latitude surface boxes. At steady state, there is a flux of carbon from the atmosphere to the high
 416 latitude surface box, while the low-latitude surface ocean releases carbon to the atmosphere.
 417



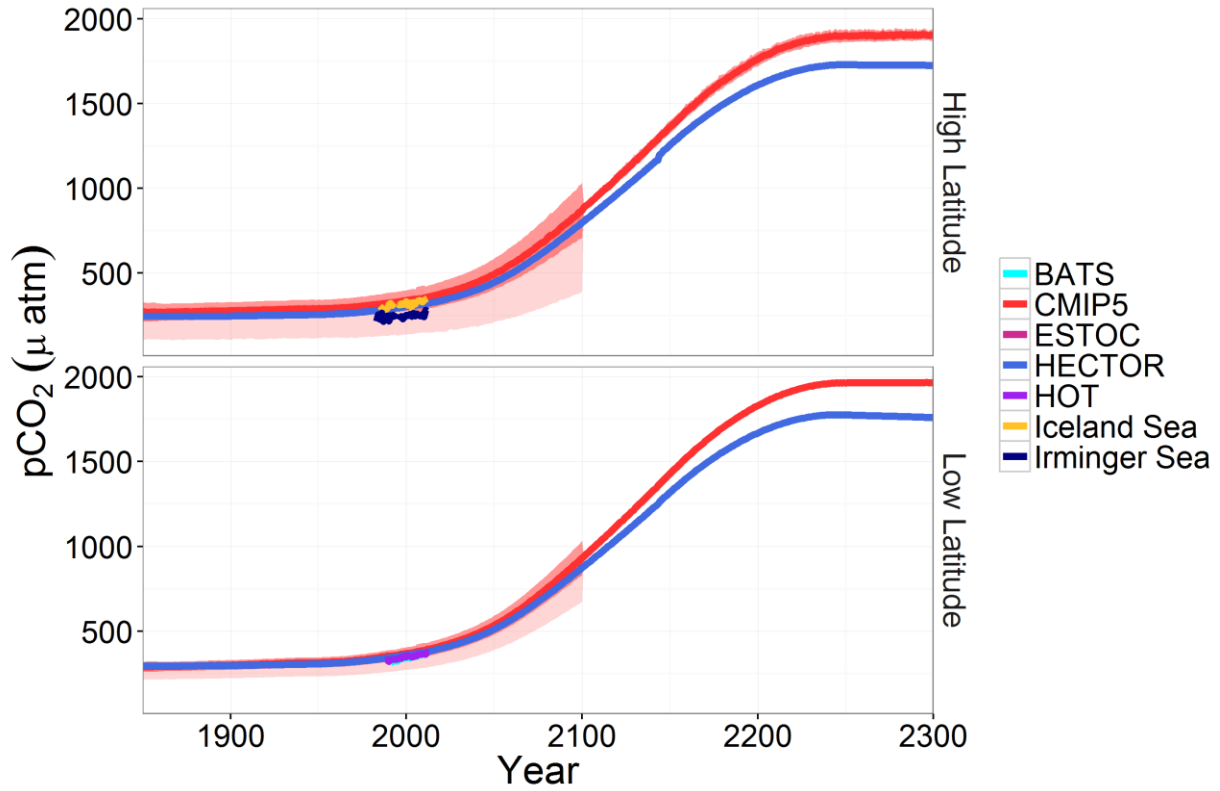
418

419 **Figure 2:** Dissolved inorganic carbon (DIC) for high (top) and low latitude (bottom) surface ocean under
420 RCP 8.5; Hector (blue), CMIP5 median, standard deviation, and model range (red, $n = 15$ (1850-2100,
421 with $n=4$ starting after 1860) and $n= 3$ (2101-2300)); and observations from BATS (teal), ESTOC (pink),
422 HOT (purple), Iceland (yellow) and Irminger Sea (navy). Note a doubling of CO_2 from preindustrial values
423 occurs around 2050.
424



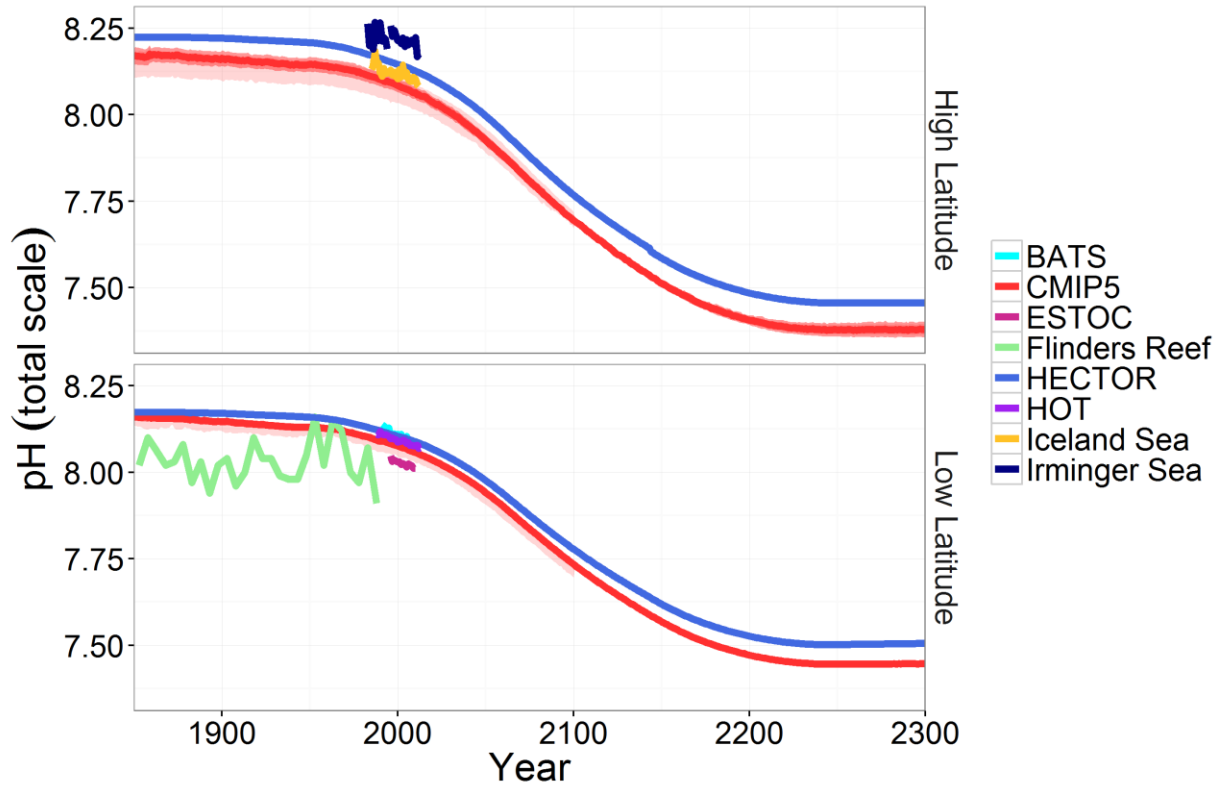
425

426 **Figure 3:** pCO₂ for high (top) and low latitude (bottom) surface ocean under RCP 8.5; Hector (blue),
427 CMIP5 median, standard deviation, and model range (red, $n = 15$ (1850-2100) and $n = 2$ (2101-2300));
428 and observations from BATS (teal), HOT (purple), ESTOC (pink), Iceland (yellow) and Irminger Sea (navy).



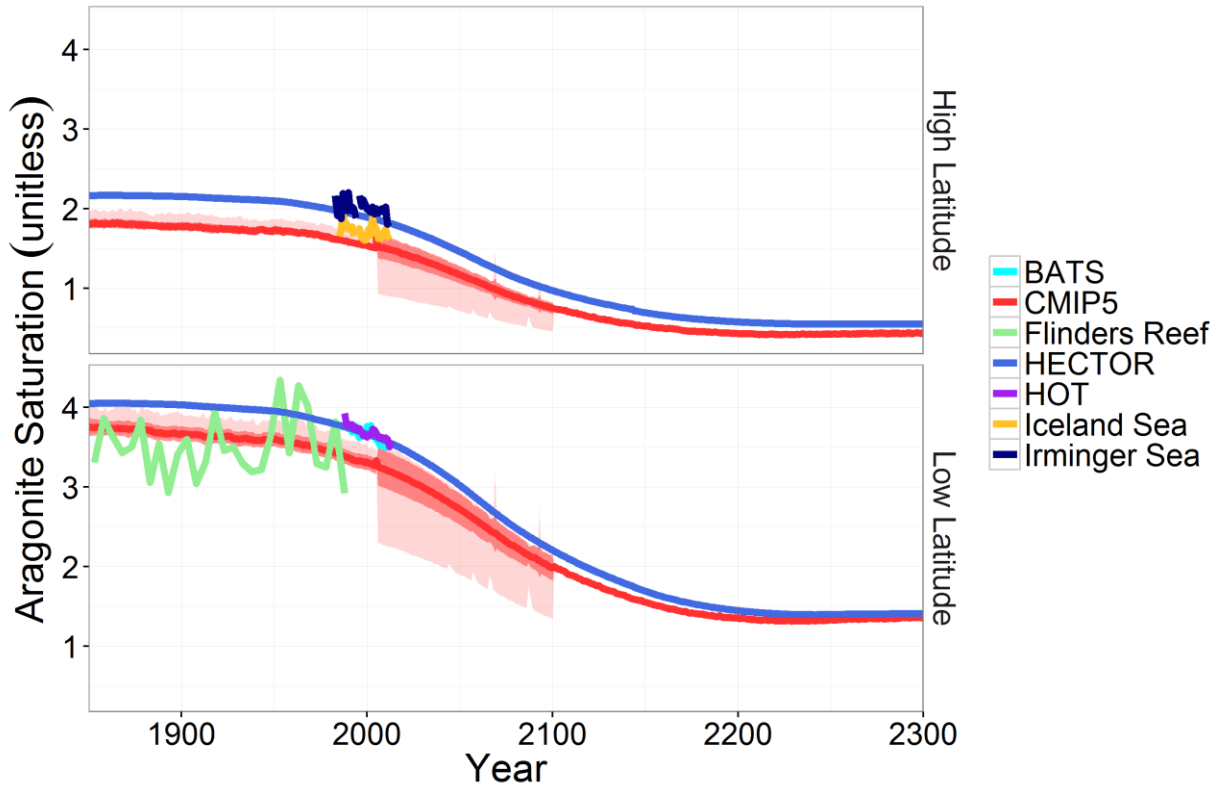
429

430 **Figure 4:** pH for high (top) and low latitude (bottom) surface ocean under RCP 8.5; Hector (blue), CMIP5
 431 median, standard deviation, and model range (red, $n = 13$ (1850-2100) and $n= 2$ (2101-2300)); and
 432 observations from BATS (teal), ESTOC (pink), HOT (purple) Flinder's Reef (green), Iceland (yellow) and
 433 Irminger Sea (navy).



434

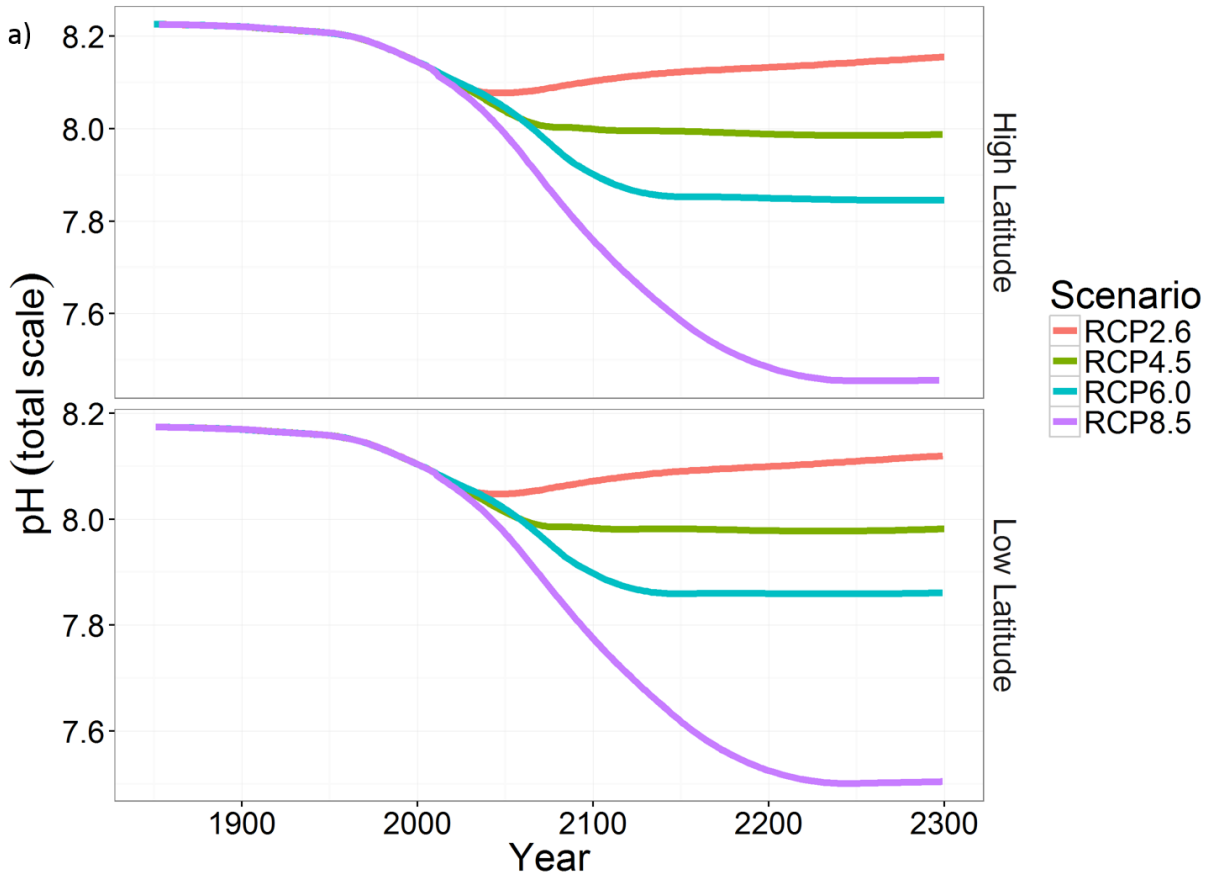
435 **Figure 5:** Aragonite saturation (Ω_{Ar}) for high (top) and low latitude (bottom) surface ocean under RCP
 436 8.5; Hector (blue), CMIP5 median, standard deviation, and model range (red, $n = 10$ (1850-2100) and $n=$
 437 2 (2101-2300)); and observations from BATS (teal), HOT (purple) and Flinders Reef (green).



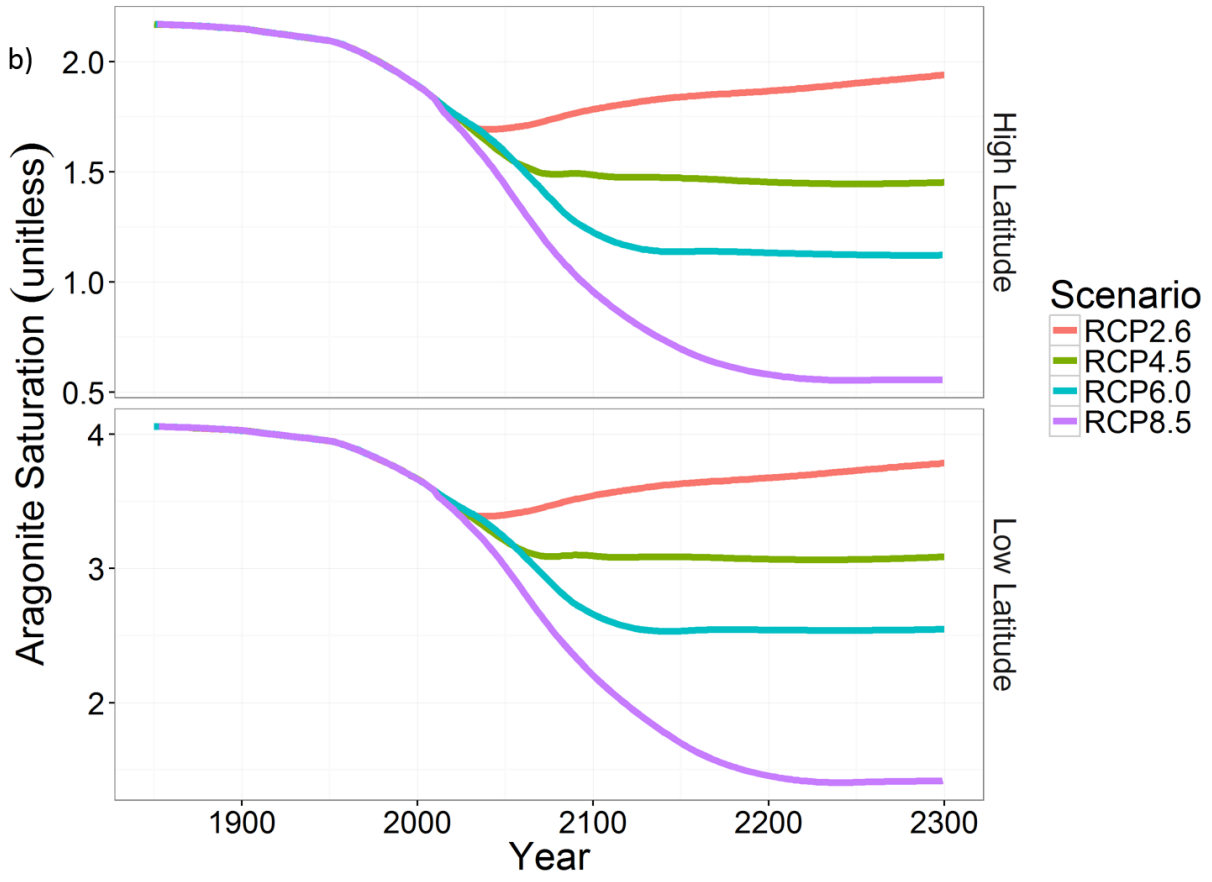
438

439

440 **Figure 6:** High and low latitude a) pH and b) aragonite saturation (Ω_{Ar}) time series for Hector from 1850-
441 2300 for RCP 2.6 (red), RCP 4.5 (green), RCP 6.0 (teal) and RCP 8.5 (purple). Note that even under a
442 strongly mitigated scenario (RCP 2.6), both Ω_{Ar} and pH at 2300 are still lower than preindustrial values.



443



444

445

446 REFERENCES

- 447 Albright, R., Langdon, C., and Anthony, K. R. N.: Dynamics of seawater carbonate chemistry, production,
448 and calcification of a coral reef flat, central Great Barrier Reef, *Biogeosciences*, 10, 6747-6758,
449 10.5194/bg-10-6747-2013, 2013.
- 450 Archer, D., Eby, M., Brovkin, V., Ridgwell, A., Cao, L., Mikolajewicz, U., Caldeira, K., Matsumoto, K.,
451 Munhoven, G., Montenegro, A., and Tokos, K.: Atmospheric Lifetime of Fossil Fuel Carbon Dioxide,
452 *Annual Review of Earth and Planetary Sciences*, 37, 117-134,
453 doi:10.1146/annurev.earth.031208.100206, 2009.
- 454 Bates, N. R.: Interannual variability of the oceanic CO₂ sink in the subtropical gyre of the North Atlantic
455 Ocean over the last 2 decades, *Journal of Geophysical Research: Oceans*, 112, C09013,
456 10.1029/2006JC003759, 2007.
- 457 Bates, N. R., Astor, Y. M., Church, M. J., Currie, K., Dore, J. E., Gonzalez-Davila, M., Lorenzoni, L., Muller-
458 Karger, F., Olafsson, J., and Santana-Casiano, J. M.: A time-series view of changing ocean chemistry due
459 to ocean uptake of anthropogenic CO₂ and ocean acidification, *Oceanography*, 27, 126-141,
460 <http://dx.doi.org/10.5670/oceanog.2014.16>, 2014.
- 461 Bopp, L., Resplandy, L., Orr, J. C., Doney, S. C., Dunne, J. P., Gehlen, M., Halloran, P., Heinze, C., Ilyina, T.,
462 Séférian, R., Tjiputra, J., and Vichi, M.: Multiple stressors of ocean ecosystems in the 21st century:
463 projections with CMIP5 models, *Biogeosciences Discuss.*, 10, 3627-3676, 10.5194/bgd-10-3627-2013,
464 2013.
- 465 Byrne, R. H., Mecking, S., Feely, R. A., and Liu, X.: Direct observations of basin-wide acidification of the
466 North Pacific Ocean, *Geophysical Research Letters*, 37, L02601, 10.1029/2009GL040999, 2010.
- 467 Caldeira, K., Jain, A. K., and Hoffert, M. I.: Climate Sensitivity Uncertainty and the Need for Energy
468 Without CO₂ Emission, *Science*, 299, 2052-2054, 10.1126/science.1078938, 2003.
- 469 Cheng, W., Chiang, J. C. H., and Zhang, D.: Atlantic Meridional Overturning Circulation (AMOC) in CMIP5
470 Models: RCP and Historical Simulations, *Journal of Climate*, 26, 7187-7197, 10.1175/JCLI-D-12-00496.1,
471 2013.
- 472 Cooley, S. R., and Doney, S. C.: Anticipating ocean acidification's economic consequences for commercial
473 fisheries, *Environmental Research Letters*, 4, 024007, 2009.
- 474 Davidson, E. A., and Janssens, I. A.: Temperature sensitivity of soil carbon decomposition and feedbacks
475 to climate change, *Nature*, 440, 165-173, 2006.
- 476 Dickson, A. G., and Millero, F. J.: A comparison of the equilibrium constants for the dissociation of
477 carbonic acid in seawater media, *Deep Sea Research Part A. Oceanographic Research Papers*, 34, 1733-
478 1743, [http://dx.doi.org/10.1016/0198-0149\(87\)90021-5](http://dx.doi.org/10.1016/0198-0149(87)90021-5), 1987.
- 479 DOE: Handbook of methods for the analysis of the various parameters of the carbon dioxide system in
480 sea water, edited by: Dickson, A. G., and Goyet, C., ORNL/CDIAC-74, 1994.
- 481 Doney, S. C.: The Growing Human Footprint on Coastal and Open-Ocean Biogeochemistry, *Science*, 328,
482 1512-1516, 10.1126/science.1185198, 2010.
- 483 Dore, J. E., Lukas, R., Sadler, D. W., Church, M. J., and Karl, D. M.: Physical and biogeochemical
484 modulation of ocean acidification in the central North Pacific, *Proceedings of the National Academy of
485 Sciences*, 106, 12235-12240, 10.1073/pnas.0906044106, 2009.
- 486 Eglinton, T. I., and Repeta, D. J.: Organic Matter in the Contemporary Ocean, *Treatise on Geochemistry*,
487 edited by: Holland, H. D., and Turekian, K. K., Elsevier, Amsterdam, 2004.
- 488 Ekstrom, J. A., Suatoni, L., Cooley, S. R., Pendleton, L. H., Waldbusser, G. G., Cinner, J. E., Ritter, J.,
489 Langdon, C., van Hooijdonk, R., Gledhill, D., Wellman, K., Beck, M. W., Brander, L. M., Rittschof, D.,
490 Doherty, C., Edwards, P. E. T., and Portela, R.: Vulnerability and adaptation of US shellfisheries to ocean
491 acidification, *Nature Clim. Change*, 5, 207-214, 10.1038/nclimate2508

492 <http://www.nature.com/nclimate/journal/v5/n3/abs/nclimate2508.html#supplementary-information>,
493 2015.

494 Fabry, V. J., Seibel, B. A., Feely, R. A., and Orr, J. C.: Impacts of ocean acidification on marine fauna and
495 ecosystem processes, *ICES Journal of Marine Science: Journal du Conseil*, 65, 414-432,
496 10.1093/icesjms/fsn048, 2008.

497 Feely, R. A., Sabine, C. L., Lee, K., Berelson, W., Kleypas, J., Fabry, V. J., and Millero, F. J.: Impact of
498 Anthropogenic CO₂ on the CaCO₃ System in the Oceans, *Science*, 305, 362-366,
499 10.1126/science.1097329, 2004.

500 Feely, R. A., Doney, S. C., and Cooley, S. R.: Ocean acidification: present conditions and future changes in
501 a high-CO₂ world, *Oceanography*, 22, 36-47, <http://dx.doi.org/10.5670/oceanog.2009.95>, 2009.

502 Feely, R. A., Sabine, C. L., Byrne, R. H., Millero, F. J., Dickson, A. G., Wanninkhof, R., Murata, A., Miller, L.
503 A., and Greeley, D.: Decadal changes in the aragonite and calcite saturation state of the Pacific Ocean,
504 *Global Biogeochemical Cycles*, 26, GB3001, 10.1029/2011GB004157, 2012.

505 Friedlingstein, P., Meinshausen, M., Arora, V. K., Jones, C. D., Anav, A., Liddicoat, S. K., and Knutti, R.:
506 Uncertainties in CMIP5 Climate Projections due to Carbon Cycle Feedbacks, *Journal of Climate*, 27, 511-
507 526, 10.1175/JCLI-D-12-00579.1, 2014.

508 Fry, C. H., Tyrrell, T., Hain, M. P., Bates, N. R., and Achterberg, E. P.: Analysis of global surface ocean
509 alkalinity to determine controlling processes, *Marine Chemistry*, 174, 46-57,
510 <http://dx.doi.org/10.1016/j.marchem.2015.05.003>, 2015.

511 Gehlen, M., Séférian, R., Jones, D. O. B., Roy, T., Roth, R., Barry, J., Bopp, L., Doney, S. C., Dunne, J. P.,
512 Heinze, C., Joos, F., Orr, J. C., Resplandy, L., Segschneider, J., and Tjiputra, J.: Projected pH reductions by
513 2100 might put deep North Atlantic biodiversity at risk, *Biogeosciences Discuss.*, 11, 8607-8634,
514 10.5194/bgd-11-8607-2014, 2014.

515 Glotter, M., Pierrehumbert, R., Elliott, J., Matteson, N., and Moyer, E.: A simple carbon cycle
516 representation for economic and policy analyses, *Climatic Change*, 126, 319-335, 10.1007/s10584-014-
517 1224-y, 2014.

518 Hansell, D. A., and Carlson, C. A.: Marine dissolved organic matter and the carbon cycle, *Oceanography*,
519 14, 41-49, 2001.

520 Hartin, C. A., Patel, P., Schwarber, A., Link, R. P., and Bond-Lamberty, B. P.: A simple object-oriented and
521 open-source model for scientific and policy analyses of the global climate system – Hector v1.0, *Geosci.*
522 *Model Dev.*, 8, 939-955, 10.5194/gmd-8-939-2015, 2015.

523 Held, I. M., and Soden, B. J.: Robust Responses of the Hydrological Cycle to Global Warming, *Journal of*
524 *Climate*, 19, 5686-5699, doi:10.1175/JCLI3990.1, 2006.

525 Hönisch, B., Hemming, N. G., Archer, D., Siddall, M., and McManus, J. F.: Atmospheric Carbon Dioxide
526 Concentration Across the Mid-Pleistocene Transition, *Science*, 324, 1551-1554,
527 10.1126/science.1171477, 2009.

528 IPCC: Climate Change 2013: The Physical Science Basis. Contribution of Working Group I to the Fifth
529 Assessment Report of the Intergovernmental Panel on Climate Change, edited by: Stocker, T. F., D. Qin,
530 G.-K. Plattner, M. Tignor, S.K. Allen, J. Boschung, A. Nauels, Y. Xia, V. Bex and P.M. Midgley Cambridge
531 University Press, Cambridge, United Kingdom and New York, NY, USA, 1535 pp., 2013.

532 Irvine, P. J., Sriver, R. L., and Keller, K.: Tension between reducing sea-level rise and global warming
533 through solar-radiation management, *Nature Clim. Change*, 2, 97-100, doi:10.1038/nclimate1351, 2012.

534 Joos, F., Plattner, G.-K., Stocker, T. F., Marchal, O., and Schmittner, A.: Global Warming and Marine
535 Carbon Cycle Feedbacks on Future Atmospheric CO₂, *Science*, 284, 464-467,
536 10.1126/science.284.5413.464, 1999.

537 Key, R. M., Kozyr, A., Sabine, C. L., Lee, K., Wanninkhof, R., Bullister, J. L., Feely, R. A., Millero, F. J.,
538 Mordy, C., and Peng, T. H.: A global ocean carbon climatology: Results from Global Data Analysis Project
539 (GLODAP), *Global Biogeochemical Cycles*, 18, GB4031, 10.1029/2004GB002247, 2004.

540 Kleypas, J. A., Buddemeier, R. W., Archer, D., Gattuso, J.-P., Langdon, C., and Opdyke, B. N.: Geochemical
541 Consequences of Increased Atmospheric Carbon Dioxide on Coral Reefs, *Science*, 284, 118-120,
542 10.1126/science.284.5411.118, 1999.

543 Knox, F., and McElroy, M. B.: Changes in Atmospheric CO₂: Influence of the Marine Biota at High
544 Latitude, *J. Geophys. Res.*, 89, 4629-4637, 10.1029/JD089iD03p04629, 1984.

545 Kump, L. R., Bralower, T. R., and Ridgwell, A. J.: Ocean Acidification in Deep Time, *Oceanography*, 22, 94-
546 107, 2009.

547 Le Quéré, C., Takahashi, T., Buitenhuis, E. T., Rödenbeck, C., and Sutherland, S. C.: Impact of climate
548 change and variability on the global oceanic sink of CO₂, *Global Biogeochemical Cycles*, 24, GB4007,
549 10.1029/2009GB003599, 2010.

550 Le Quéré, C., Andres, R. J., Boden, T., Conway, T., Houghton, R. A., House, J. I., Marland, G., Peters, G. P.,
551 van der Werf, G. R., Ahlström, A., Andrew, R. M., Bopp, L., Canadell, J. G., Ciais, P., Doney, S. C., Enright,
552 C., Friedlingstein, P., Huntingford, C., Jain, A. K., Jourdain, C., Kato, E., Keeling, R. F., Klein Goldewijk, K.,
553 Levis, S., Levy, P., Lomas, M., Poulter, B., Raupach, M. R., Schwinger, J., Sitch, S., Stocker, B. D., Viovy, N.,
554 Zaehle, S., and Zeng, N.: The global carbon budget 1959–2011, *Earth Syst. Sci. Data*, 5, 165-185,
555 10.5194/essd-5-165-2013, 2013.

556 Lenton, T. M.: Land and ocean carbon cycle feedback effects on global warming in a simple Earth system
557 model, *Tellus B*, 52, 1159-1188, 10.1034/j.1600-0889.2000.01104.x, 2000.

558 Liu, C., and Allan, R. P.: Observed and simulated precipitation responses in wet and dry regions 1850–
559 2100, *Environmental Research Letters*, 8, 034002, 2013.

560 Lueker, T. J., Dickson, A. G., and Keeling, C. D.: Ocean pCO₂ calculated from dissolved inorganic carbon,
561 alkalinity, and equations for K₁ and K₂; validation based on laboratory measurements of CO₂ in gas and
562 seawater at equilibrium, *Marine Chemistry*, 70, 105-119, 2000.

563 Matear, R. J., and Hirst, A. C.: Climate change feedback on the future oceanic CO₂ uptake, *Tellus B*, 51,
564 722-733, 10.1034/j.1600-0889.1999.t01-1-00012.x, 1999.

565 Mehrbach, C., Culbertson, C. H., Hawley, J. E., and Pytkowicz, R. M.: Measurement of the apparent
566 dissociation constants of carbonic acid in seawater at atmospheric pressure, *Limnol. Oceanogr.*, 18, 897-
567 907, 1973.

568 Millero, F. J.: Thermodynamics of the carbon dioxide system in the oceans, *Geochimica et Cosmochimica*
569 *Acta*, 59, 661-677, 10.1016/0016-7037(94)00354-O, 1995.

570 Moss, R. H., Edmonds, J. A., Hibbard, K. A., Manning, M. R., Rose, S. K., van Vuuren, D. P., Carter, T. R.,
571 Emori, S., Kainuma, M., Kram, T., Meehl, G. A., Mitchell, J. F. B., Nakicenovic, N., Riahi, K., Smith, S. J.,
572 Stouffer, R. J., Thomson, A. M., Weyant, J. P., and Wilbanks, T. J.: The next generation of scenarios for
573 climate change research and assessment, *Nature*, 463, 747-756, doi:10.1038/nature08823, 2010.

574 Mucci, A.: The solubility of calcite and aragonite in seawater at various salinities, temperatures and at
575 one atmosphere pressure, *Amer. J. of Science*, 283, 781-799, 1983.

576 Orr, J. C., Fabry, V. J., Aumont, O., Bopp, L., Doney, S. C., Feely, R. A., Gnanadesikan, A., Gruber, N.,
577 Ishida, A., Joos, F., Key, R. M., Lindsay, K., Maier-Reimer, E., Matear, R., Monfray, P., Mouchet, A., Najjar,
578 R. G., Plattner, G.-K., Rodgers, K. B., Sabine, C. L., Sarmiento, J. L., Schlitzer, R., Slater, R. D., Totterdell, I.
579 J., Weirig, M.-F., Yamanaka, Y., and Yool, A.: Anthropogenic ocean acidification over the twenty-first
580 century and its impact on calcifying organisms, *Nature*, 437, 681-686, doi:10.1038/nature04095, 2005.

581 Pelejero, C., Calvo, E., McCulloch, M. T., Marshall, J. F., Gagan, M. K., Lough, J. M., and Opdyke, B. N.:
582 Preindustrial to Modern Interdecadal Variability in Coral Reef pH, *Science*, 309, 2204-2207,
583 10.1126/science.1113692, 2005.

584 Pietsch, S. A., and Hasenauer, H.: Evaluating the self-initialization procedure for large-scale ecosystem
585 models, *Global Change Biology*, 12, 1-12, 2006.

586 Riahi, K., Rao, S., Krey, V., Cho, C., Chirkov, V., Fischer, G., Kindermann, G., Nakicenovic, N., and Rafaj, P.:
587 RCP 8.5—A scenario of comparatively high greenhouse gas emissions, *Climatic Change*, 109, 33-57,
588 10.1007/s10584-011-0149-y, 2011.

589 Ricciuto, D. M., Davis, K. J., and Keller, K.: A Bayesian calibration of a simple carbon cycle model: The role
590 of observations in estimating and reducing uncertainty, *Global Biogeochemical Cycles*, 22, GB2030,
591 10.1029/2006GB002908, 2008.

592 Ricke, K. L., Orr, J. C., Schneider, K., and Caldeira, K.: Risks to coral reefs from ocean carbonate chemistry
593 changes in recent earth system model projections, *Environmental Research Letters*, 8, 034003, doi:
594 10.1088/1748-9326/8/3/034003, 2013.

595 Riebesell, U., Zondervan, I., Rost, B., Tortell, P. D., Zeebe, R. E., and Morel, F. M. M.: Reduced
596 calcification of marine plankton in response to increased atmospheric CO₂, *Nature*, 407, 364-367, 2000.

597 Riebesell, U., Körtzinger, A., and Oschlies, A.: Sensitivities of marine carbon fluxes to ocean change,
598 *Proceedings of the National Academy of Sciences*, 106, 20602-20609, 10.1073/pnas.0813291106, 2009.

599 Riley, J. P., and Tongudai, M.: The major cation/chlorinity ratios in sea water, *Chemical Geology*, 2, 263-
600 269, [http://dx.doi.org/10.1016/0009-2541\(67\)90026-5](http://dx.doi.org/10.1016/0009-2541(67)90026-5), 1967.

601 Roy, T., Lombard, F., Bopp, L., and Gehlen, M.: Projected impacts of climate change and ocean
602 acidification on the global biogeography of planktonic Foraminifera, *Biogeosciences*, 12, 2873-2889,
603 10.5194/bg-12-2873-2015, 2015.

604 Sabine, C. L., Feely, R. A., Gruber, N., Key, R. M., Lee, K., Bullister, J. L., Wanninkhof, R., Wong, C. S.,
605 Wallace, D. W. R., Tilbrook, B., Millero, F. J., Peng, T.-H., Kozyr, A., Ono, T., and Rios, A. F.: The Oceanic
606 Sink for Anthropogenic CO₂, *Science*, 305, 367-371, 10.1126/science.1097403, 2004.

607 Sabine, C. L., Feely, R., Wanninkhof, R., Takahashi, T., Khatiwala, S., and Park, G.-H.: The global ocean
608 carbon cycle, In *State of the Climate in 2010*, *Global Oceans. Bull. Am. Meteorol. Soc.*, 92, S100-S108,
609 10.1175/1520-0477-92.6.S1, 2011.

610 Sarmiento, J. L., and Toggweiler, J. R.: A new model for the role of the oceans in determining
611 atmospheric PCO₂, *Nature*, 308, 621-624, 1984.

612 Sarmiento, J. L., and Le Quéré, C.: Oceanic Carbon Dioxide Uptake in a Model of Century-Scale Global
613 Warming, *Science*, 274, 1346-1350, 10.1126/science.274.5291.1346, 1996.

614 Sarmiento, J. L., and Gruber, N.: *Ocean Biogeochemical Dynamics*, edited by: Press, P. U., Princeton NJ,
615 2006.

616 Sasse, T. P., McNeil, B. I., Matear, R. J., and Lenton, A.: Quantifying the influence of CO₂ seasonality on
617 future aragonite undersaturation onset, *Biogeosciences*, 12, 6017-6031, 10.5194/bg-12-6017-2015,
618 2015.

619 Senior, C. A., and Mitchell, J. F. B.: The time-dependence of climate sensitivity, *Geophysical Research*
620 *Letters*, 27, 2685-2688, 10.1029/2000GL011373, 2000.

621 Siegenthaler, U., and Joos, F.: Use of a simple model for studying oceanic tracer distributions and the
622 global carbon cycle, *Tellus B*, 44, 186-207, 10.1034/j.1600-0889.1992.t01-2-00003.x, 1992.

623 Silverman, J., Lazar, B., Cao, L., Caldeira, K., and Erez, J.: Coral reefs may start dissolving when
624 atmospheric CO₂ doubles, *Geophysical Research Letters*, 36, n/a-n/a, 10.1029/2008GL036282, 2009.

625 Takahashi, T., Sutherland, S. C., Wanninkhof, R., Sweeney, C., Feely, R. A., Chipman, D. W., Hales, B.,
626 Friederich, G., Chavez, F., Sabine, C., Watson, A., Bakker, D. C. E., Schuster, U., Metzl, N., Yoshikawa-
627 Inoue, H., Ishii, M., Midorikawa, T., Nojiri, Y., Körtzinger, A., Steinhoff, T., Hoppema, M., Olafsson, J.,
628 Arnarson, T. S., Tilbrook, B., Johannessen, T., Olsen, A., Bellerby, R., Wong, C. S., Delille, B., Bates, N. R.,
629 and de Baar, H. J. W.: Climatological mean and decadal change in surface ocean pCO₂, and net sea-air
630 CO₂ flux over the global oceans, *Deep Sea Research Part II: Topical Studies in Oceanography*, 56, 554-
631 577, <http://dx.doi.org/10.1016/j.dsr2.2008.12.009>, 2009.

632 Taylor, K. E., Stouffer, R. J., and Meehl, G. A.: An Overview of CMIP5 and the Experiment Design, *Bulletin*
633 *of the American Meteorological Society*, 93, 485-498, 10.1175/BAMS-D-11-00094.1, 2012.

634 van Vuuren, D., Elzen, M. J., Lucas, P., Eickhout, B., Strengers, B., Ruijven, B., Wonink, S., and Houdt, R.:
635 Stabilizing greenhouse gas concentrations at low levels: an assessment of reduction strategies and costs,
636 Climatic Change, 81, 119-159, 10.1007/s10584-006-9172-9, 2007.
637 Wanninkhof, R.: Relationship between wind speed and gas exchange over the ocean, Journal of
638 Geophysical Research: Oceans, 97, 7373-7382, 10.1029/92JC00188, 1992.
639 Weiss, R. F.: Carbon dioxide in water and seawater: the solubility of a non-ideal gas, Marine Chemistry,
640 2, 203-215, 10.1016/0304-4203(74)90015-2, 1974.
641 Woosley, R. J., Millero, F. J., and Wanninkhof, R.: Rapid anthropogenic changes in CO₂ and pH in the
642 Atlantic Ocean: 2003–2014, Global Biogeochemical Cycles, 30, 70-90, 10.1002/2015GB005248, 2016.
643 Wullschleger, S. D., Post, W. M., and King, A. W.: On the Potential for a CO₂ Fertilization Effect in
644 Forests: Estimates of the Biotic Growth Factor, Based on 58 Controlled-Exposure Studies, Biotic
645 Feedbacks in the Global Climate System: Will the Warming Feed the Warming?, edited by: G.M., W., and
646 F.T., M., Oxford University, New York, 1995.
647 Yates, K., and Halley, R.: CO₂ concentration and pCO₂ thresholds for calcification and dissolution on
648 the Molokai reef flat, Hawaii, Biogeosciences Discussions, 3, 123-154, 2006.
649 Zeebe, R. E., and Wolf-Gladrow, D.: CO₂ in Seawater: Equilibrium, Kinetics, Isotopes, Elsevier,
650 Amsterdam, 2001.

651

652